

## Improving On-stream Stability of Cu-SiO<sub>2</sub> Catalysts in the Dehydrogenation of Bioethanol to Acetaldehyde

*Giovanni Pampararo<sup>1</sup>, Zuzana Hlavenkova<sup>2</sup>, Ales Styskalik<sup>3</sup>, Damien P. Debecker<sup>1\*</sup>*

1. Université catholique de Louvain (UCLouvain), Institute of Condensed Matter and Nanosciences (IMCN), Place Louis Pasteur 1, Louvain-la-Neuve, 1348, Belgium
2. CEITEC, Masaryk University, Kamenice 5, CZ-62500 Brno, Czech Republic
3. Department of Chemistry, Masaryk University, Kotlarska 2, CZ-61137 Brno, Czech Republic

\*damien.debecker@uclouvain.be

ELECTRONIC SUPPLEMENTARY INFORMATION

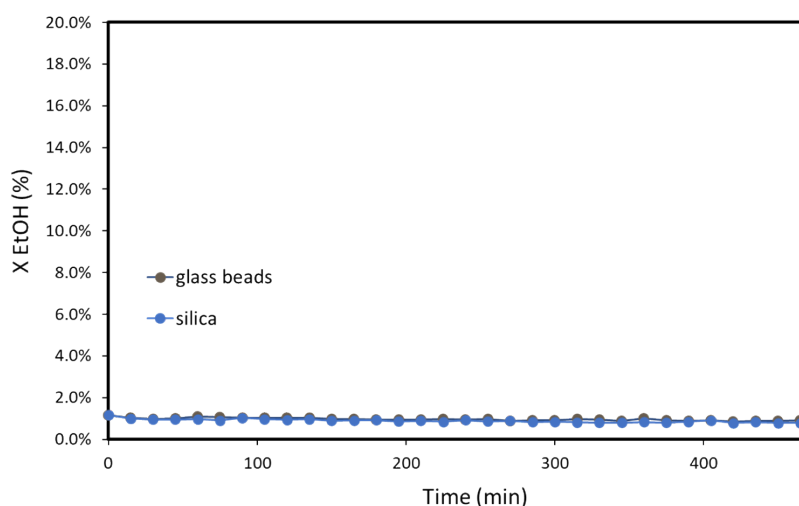


Figure S1: Catalytic test for an inert reactor (glass beads) and aerosol made silica. Test conditions: 573 K, 8 hours, constant ethanol feed, WHSV 4.02 h<sup>-1</sup>.

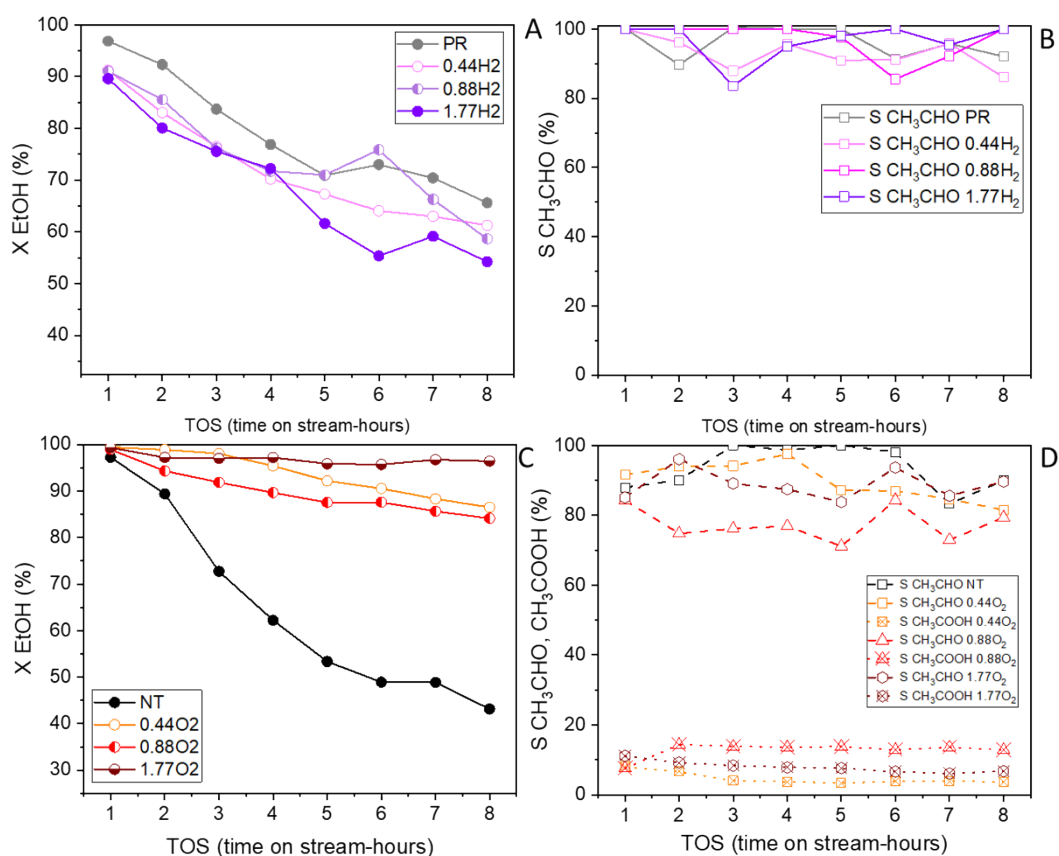


Figure S2: Ethanol conversion (A, C) and products selectivity (B, D) obtained during 8 hours stability tests. 573 K, WHSV 4.02 h<sup>-1</sup>, constant ethanol feed, tot flow 120 mL/min. Diethyl ether (C<sub>4</sub>H<sub>10</sub>O) selectivity is 0.5-0.6%, it is constant during the test and it has been removed from the graph to help the reader. When oxygen is introduced in the feed, a correspondent

reduction in the carbon balance has been observed: this can be due to concomitant formation of  $\text{CO}_x$  (not quantified)

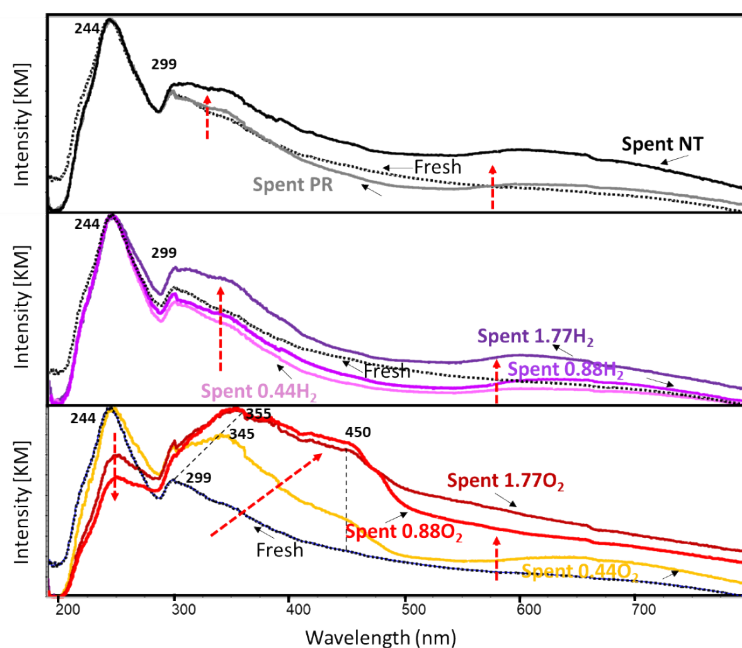


Figure S3: DR-UV-VIS spectroscopy for as synthesized catalyst and spent catalysts after 8 hours reaction under the different test conditions.

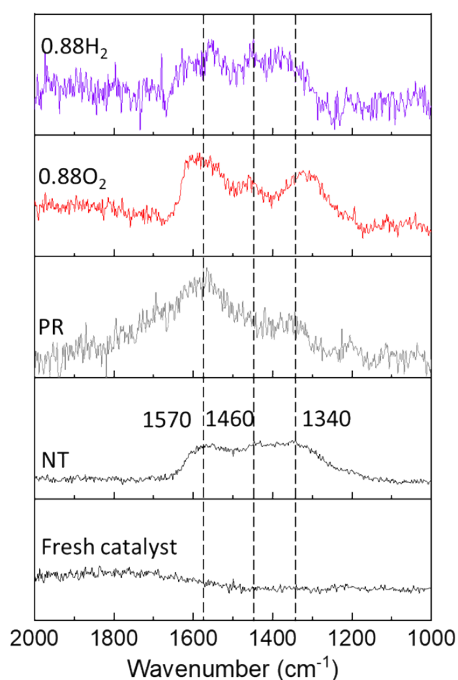


Figure S4: Raman spectra of selected catalysts, dotted lines at 1570 and 1340  $\text{cm}^{-1}$  mark the G and D band of graphitic carbon with nanometric domain. Line at 1460  $\text{cm}^{-1}$  shows amorphous carbon.

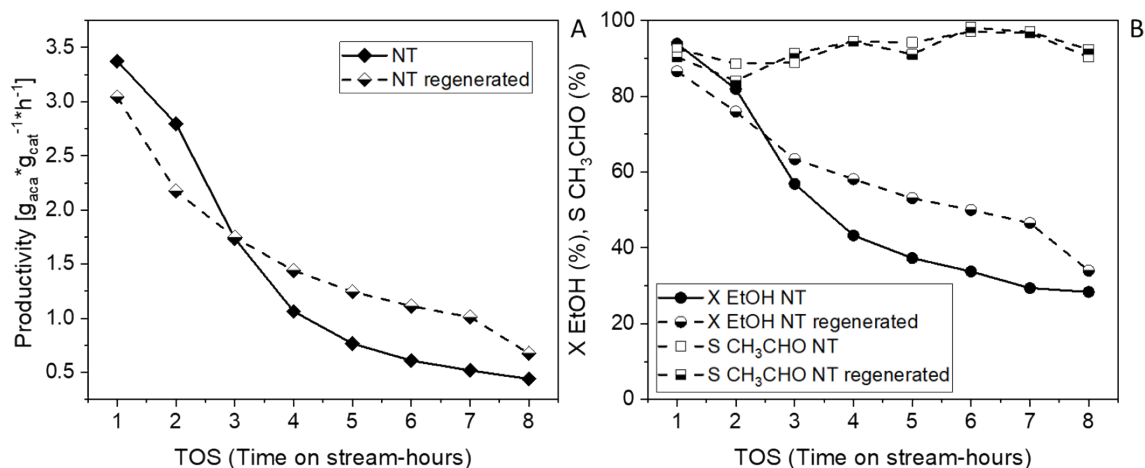


Figure S5: regeneration test over NT catalyst. Panel A report the acetaldehyde productivity while ethanol conversion and acetaldehyde selectivity are reported in panel B. Diethyl ether selectivity is the only detected by product, its selectivity is close to 1%.

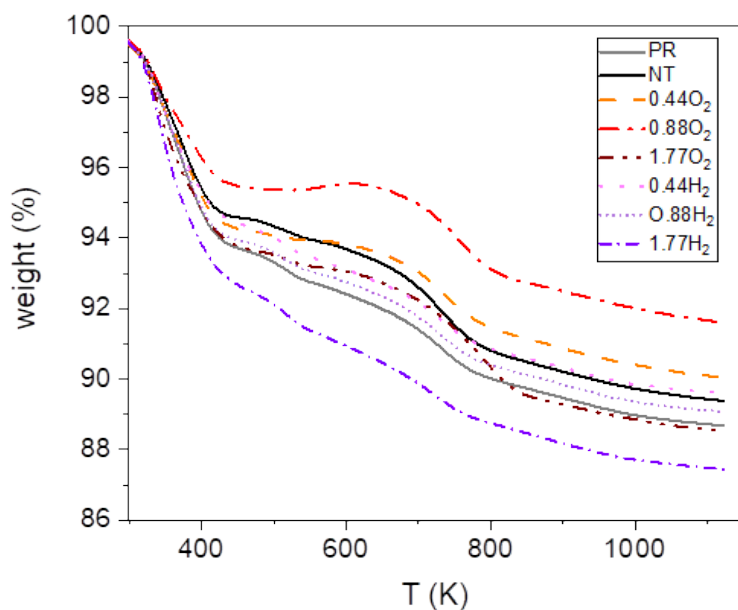


Figure S6: TG curves for the spent catalysts after 8 hours TOS. Overall mass losses are reported in Table S1. In some cases, a slight regains in weight due to the re-oxidation of Cu<sup>0</sup> and Cu<sub>2</sub>O species to CuO, can be envisaged. However this effect is moderate and doesn't affect significantly the global evaluation on mass losses.

Table S1: overall mass losses evaluated by TGA profiles

<i>Spent catalyst</i>	<i>Overall TGA mass loss (%)</i>
PR	11.3
NT	10.6
0.44H <sub>2</sub>	11.0
0.88H <sub>2</sub>	10.4
1.77H <sub>2</sub>	12.5
0.44O <sub>2</sub>	10.0
0.88O <sub>2</sub>	8.5
1.77O <sub>2</sub>	11.5
NT 24h	10.0
0.44O <sub>2</sub> 24h	9.0
1.77O <sub>2</sub> 24h	12.0
1.77H <sub>2</sub> 24h	9.5

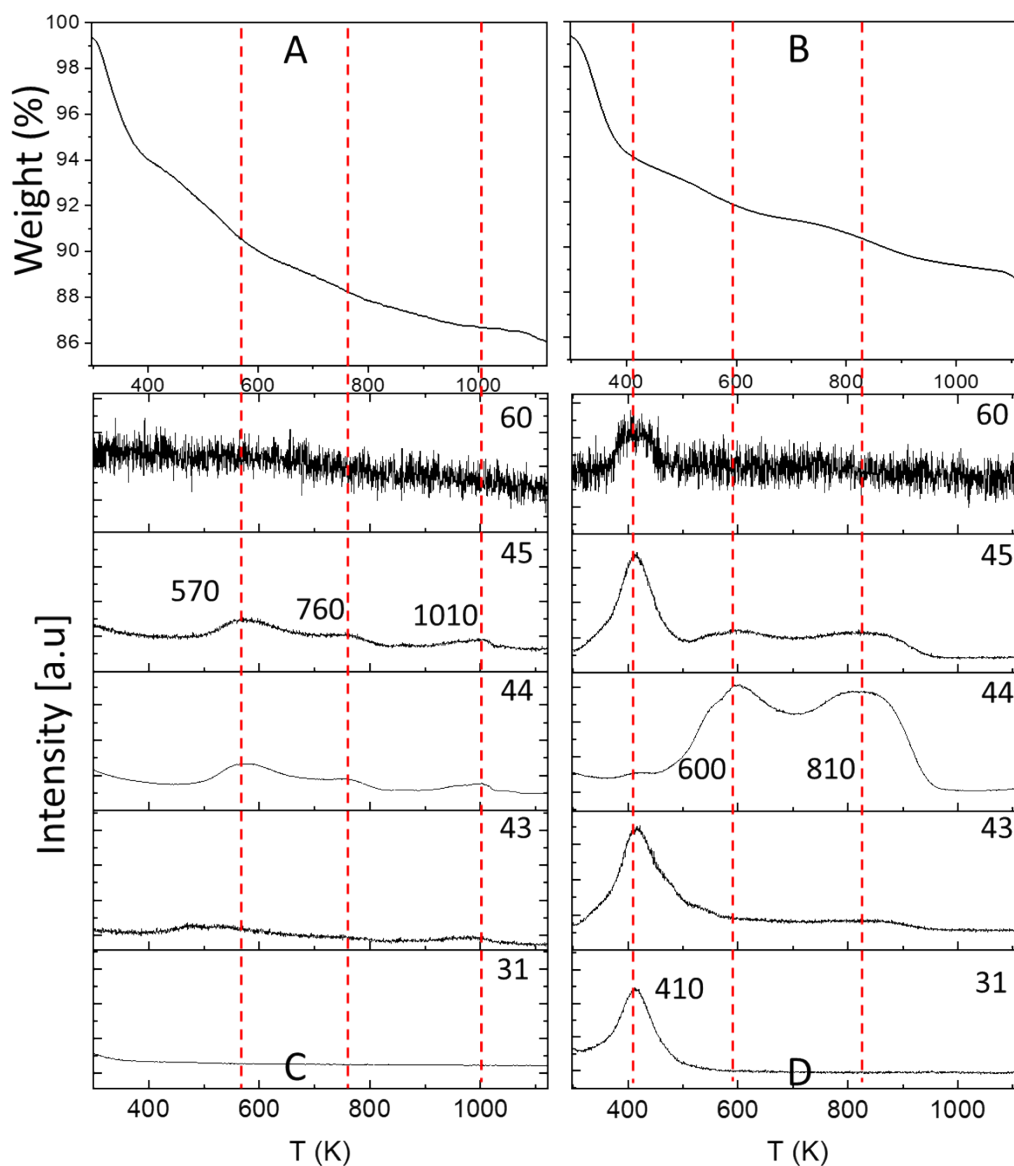


Figure S7: TGA-MS analyses carried out under  $N_2$  flow on NT (left) and  $0.88O_2$  (right). TGA profiles are reported in panels A, B. MS profiles are reported in panels C, D for  $m/z = 31, 43, 44, 45,$  and  $60$ .

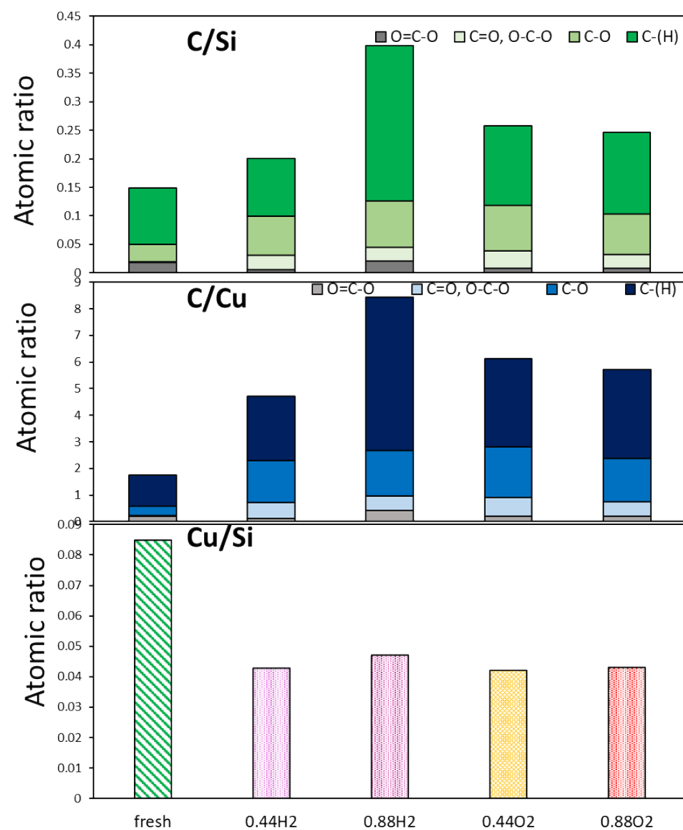


Figure S8: C/Si, C/Cu and Cu/Si atomic ratio for  $0.44H_2, 0.88H_2, 0.44O_2, 0.88O_2$ .

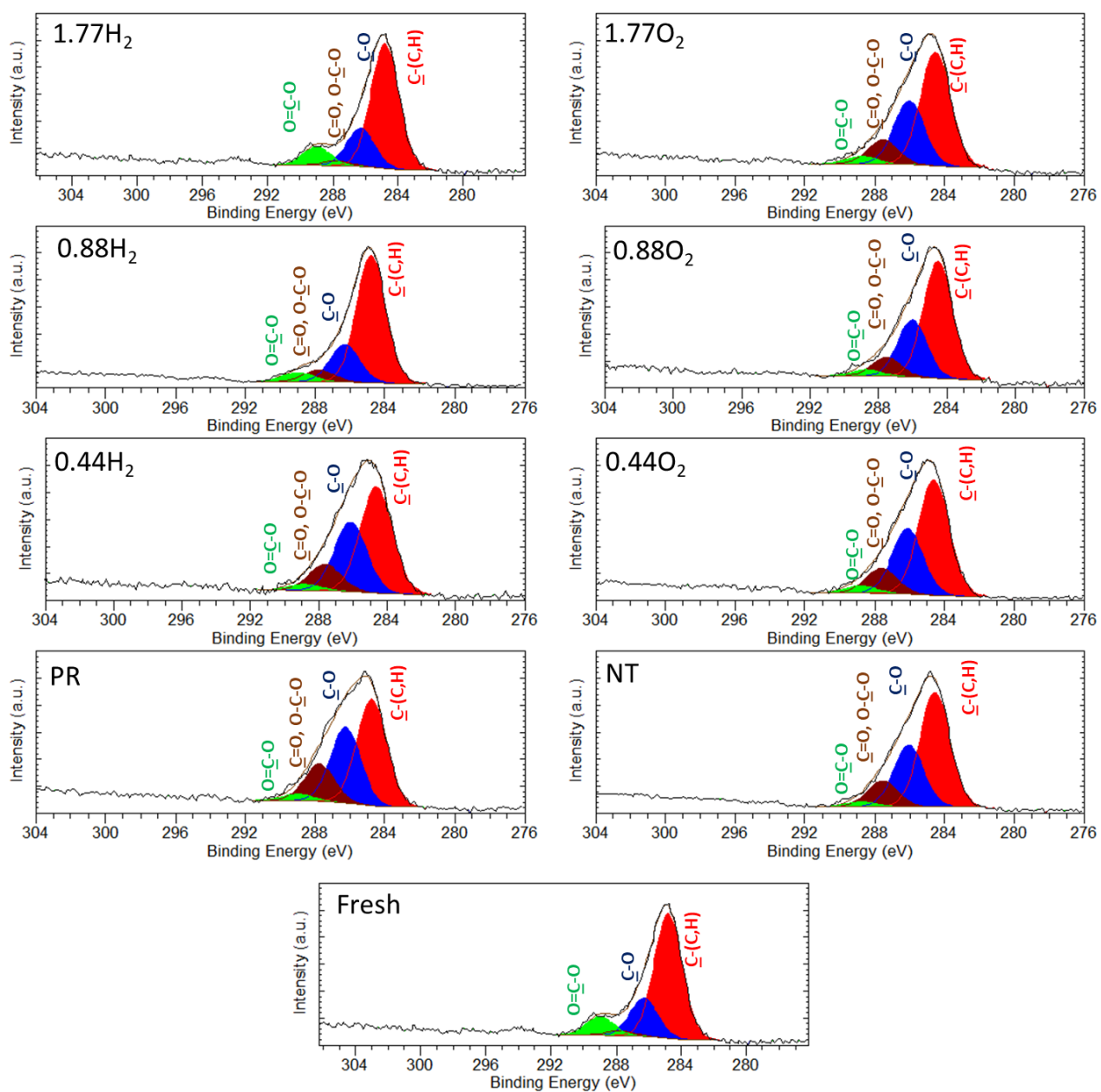


Figure S9: C1s High resolution spectra for both fresh and spent catalysts after 8 h TOS.

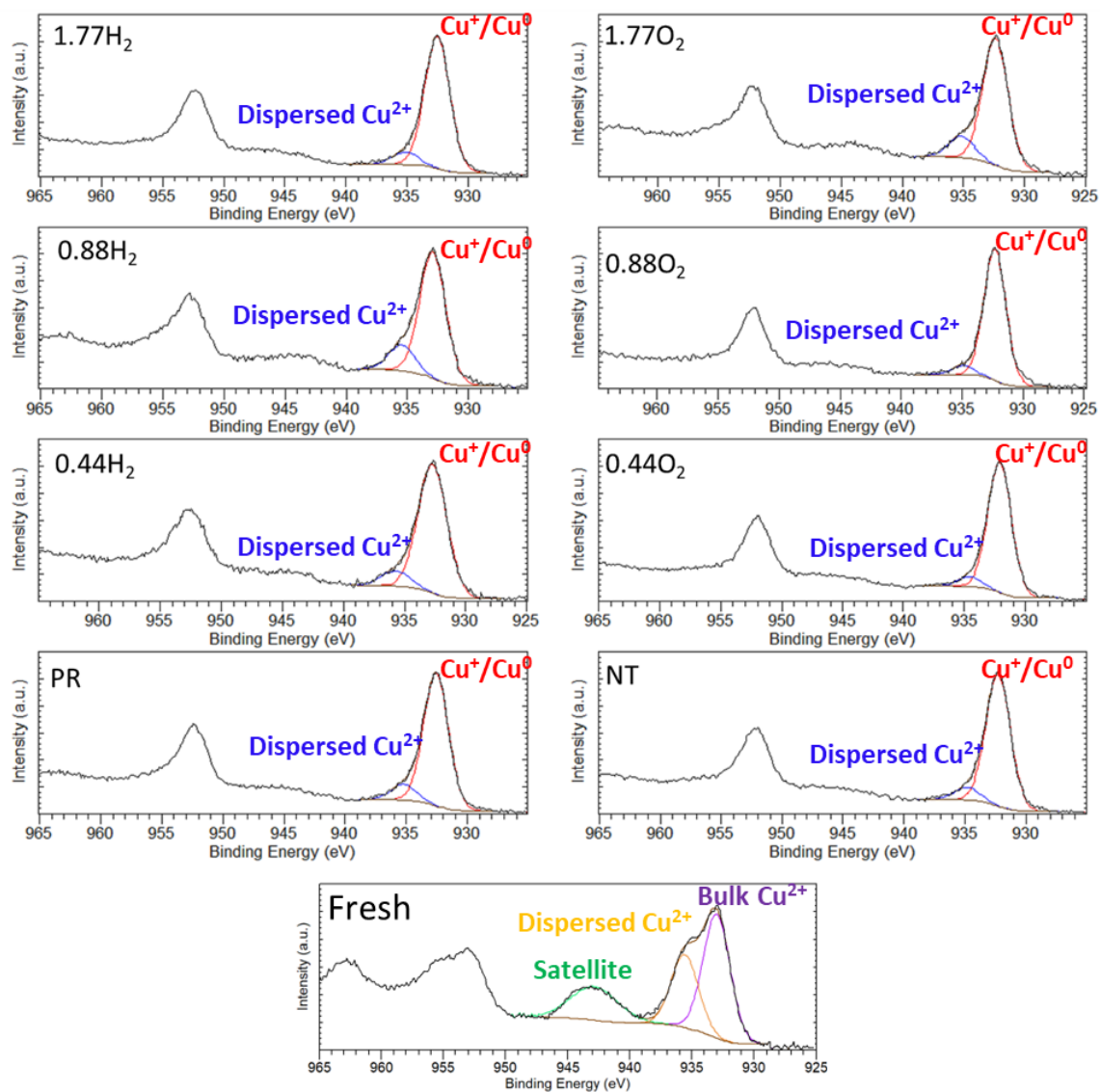


Figure S10: Cu 2p XPS high resolution spectra of fresh and spent catalysts after 8h TOS.



Table S2: Relative intensity (averaged on three measurements) of the relevant clusters detected in the ToF-SiMS experiment.

Fragments	Fresh	NT	PR	1.77H <sub>2</sub>	1.77O <sub>2</sub>
CH <sub>3</sub> <sup>+</sup>	0.0079 ± 0.0002	0.0081 ± 0.0005	0.0101 ± 0.0001	0.0073 ± 0.0008	0.0086 ± 0.0001
H <sub>3</sub> O <sup>+</sup>	0.0014 ± 0.0001	0.0013 ± 0.0000	0.0012 ± 0.0000	0.0010 ± 0.0001	0.0012 ± 0.0001
Si <sup>+</sup>	0.0418 ± 0.0026	0.0217 ± 0.0030	0.0440 ± 0.0025	0.0259 ± 0.0045	0.0385 ± 0.0079
CHO <sup>+</sup>	0.0071 ± 0.0001	0.0069 ± 0.0005	0.0087 ± 0.0000	0.0065 ± 0.0006	0.0069 ± 0.0001
SiHO <sup>+</sup>	0.0595 ± 0.0007	0.0408 ± 0.0037	0.0657 ± 0.0008	0.0432 ± 0.0050	0.0539 ± 0.0040
Cu <sup>+</sup>	0.0146 ± 0.0008	0.0232 ± 0.0005	0.0183 ± 0.0019	0.0157 ± 0.0006	0.0199 ± 0.0009
<sup>65</sup> Cu <sup>+</sup>	0.0066 ± 0.0003	0.0103 ± 0.0002	0.0082 ± 0.0008	0.0070 ± 0.0003	0.0089 ± 0.0003
C <sub>4</sub> H <sub>5</sub> <sup>+</sup>	0.0108 ± 0.0006	0.0113 ± 0.0005	0.0113 ± 0.0002	0.0139 ± 0.0004	0.0108 ± 0.0004
C <sub>4</sub> H <sub>3</sub> <sup>+</sup>	0.0058 ± 0.0003	0.0059 ± 0.0002	0.0066 ± 0.0002	0.0076 ± 0.0005	0.0059 ± 0.0004
C <sub>3</sub> H <sub>7</sub> O <sup>+</sup>	0.0046 ± 0.0002	0.0051 ± 0.0002	0.0047 ± 0.0004	0.0049 ± 0.0004	0.0047 ± 0.0001
C <sub>4</sub> H <sub>7</sub> O <sup>+</sup>	0.0064 ± 0.0001	0.0070 ± 0.0002	0.0068 ± 0.0004	0.0063 ± 0.0008	0.0069 ± 0.0002
C <sub>6</sub> H <sub>5</sub> <sup>+</sup>	0.0043 ± 0.0003	0.0040 ± 0.0001	0.0049 ± 0.0002	0.0057 ± 0.0004	0.0043 ± 0.0003
C <sub>3</sub> H <sub>5</sub> O <sub>3</sub> <sup>+</sup>	0.0007 ± 0.0000	0.0006 ± 0.0000	0.0007 ± 0.0000	0.0008 ± 0.0001	0.0007 ± 0.0001
Si <sub>2</sub> O <sub>2</sub> <sup>+</sup>	0.0020 ± 0.0000	0.0012 ± 0.0002	0.0026 ± 0.0001	0.0013 ± 0.0002	0.0018 ± 0.0002
C <sub>7</sub> H <sub>7</sub> <sup>+</sup>	0.0045 ± 0.0003	0.0039 ± 0.0000	0.0048 ± 0.0002	0.0055 ± 0.0003	0.0045 ± 0.0004
SiH <sub>3</sub> O <sub>3</sub> <sup>+</sup>	0.0075 ± 0.0001	0.0067 ± 0.0003	0.0084 ± 0.0001	0.0068 ± 0.0004	0.0072 ± 0.0005
C <sub>8</sub> H <sub>9</sub> <sup>+</sup>	0.0016 ± 0.0003	0.0010 ± 0.0001	0.0017 ± 0.0002	0.0017 ± 0.0001	0.0015 ± 0.0003
C <sub>9</sub> H <sub>7</sub> <sup>+</sup>	0.0015 ± 0.0001	0.0011 ± 0.0001	0.0017 ± 0.0001	0.0018 ± 0.0003	0.0015 ± 0.0002
C <sub>10</sub> H <sub>19</sub> O <sup>+</sup>	0.0107 ± 0.0005	0.0093 ± 0.0010	0.0084 ± 0.0003	0.0066 ± 0.0020	0.0111 ± 0.0007

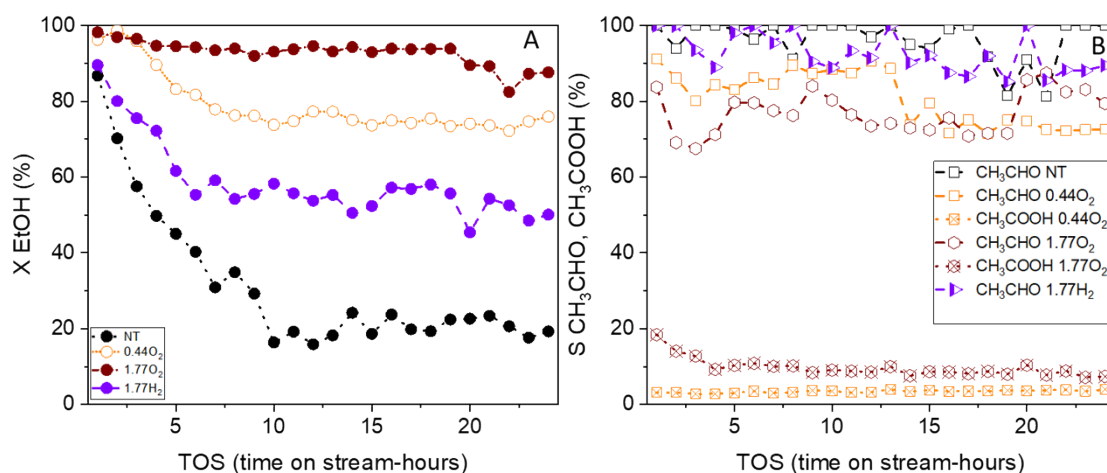


Figure S11: Ethanol conversion (A, C) and products selectivity (B, D) obtained during 24 hours stability tests. 573 K, WHSV 4.02 h<sup>-1</sup>, constant ethanol feed, tot flow 120 mL/min. Diethyl ether (C<sub>4</sub>H<sub>10</sub>O) selectivity is 0.5-0.6%, it is constant during the test and it has been removed from the graph to help the reader. When oxygen is introduced in the feed, a slight decrease in the carbon balance (down to ~80%) has been observed: this can be due to concomitant formation of CO<sub>x</sub> (not quantified here).

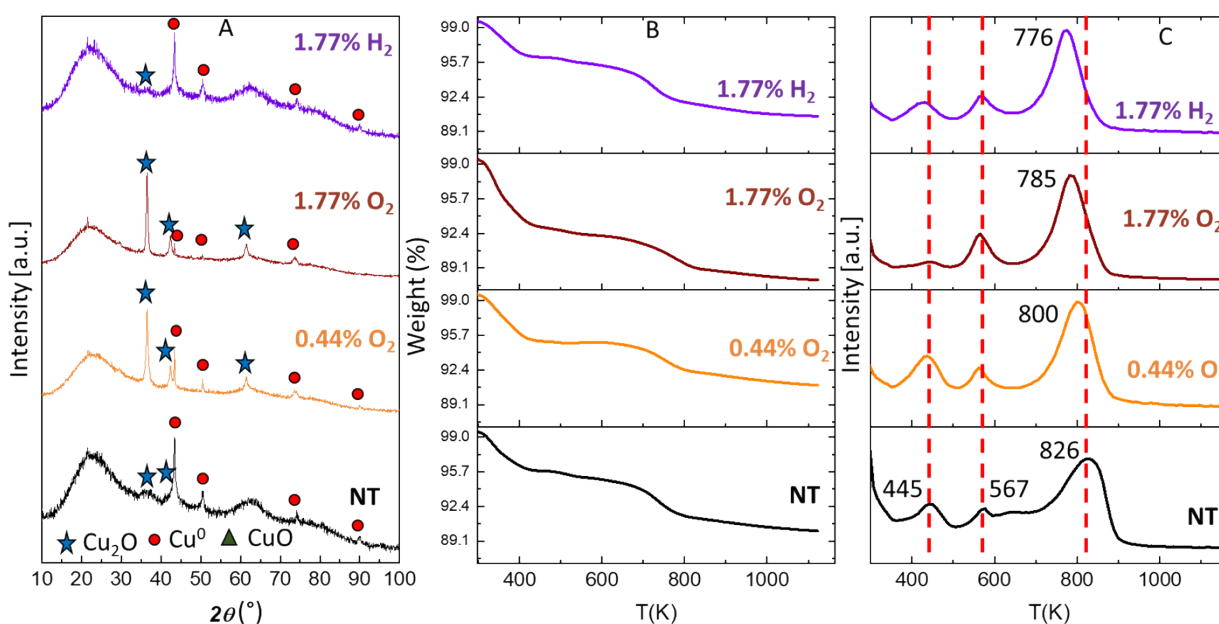


Figure S12: Characterization survey for spent catalysts after 24 hours reactions. Panel A refers to XRD patterns; panel B refers to TG curves, Panel C refers to MS profiles for fragment  $m/z = 44$  ( $\text{CO}_2$ )

XRD patterns (Fig. S12) revealed that  $\text{Cu}^0$  and  $\text{Cu}_2\text{O}$  are always the main crystalline phases detected. Approximately no change of the crystal sizes is observed between 8 hours and 24 hours, underlining the copper sintering effect as a marginal phenomenon, particularly limited to the first hours of reaction where the main deactivation occurs. TGA curves (panel B, Fig. S12) are comparable with previous ones, confirming that amount of coke doesn't change upon time (see table S1 for overall mass losses). MS profiles related to the  $\text{CO}_2$   $m/z$  fragment confirm the presence of the three previously described peaks.

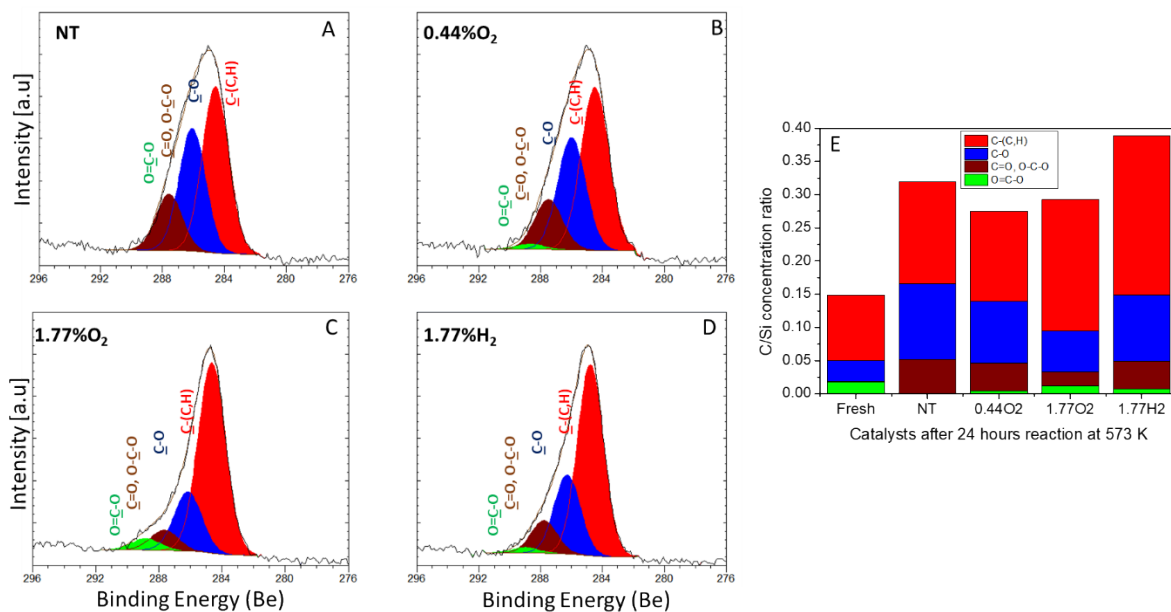


Figure S13: C1s High resolution spectra for the investigated catalysts after 24 hours TOS (A-D) and relative quantification (E) showing C/Si atomic ratio.

XPS analyses (ESI Fig. S13, panels A-D) confirmed an increased carbon amount after the catalytic tests, with similar ratios of the different carbonaceous species to those ones found over spent catalysts after 8 hours on stream, as shown in panel E. To sum up, these characterizations led us to confirm as the catalysts are mainly stabilized after either 24 or 8 hours. No further sintering occurred, underlining thermal stability of the catalysts and moreover, type and quantity of coke remain unaltered.

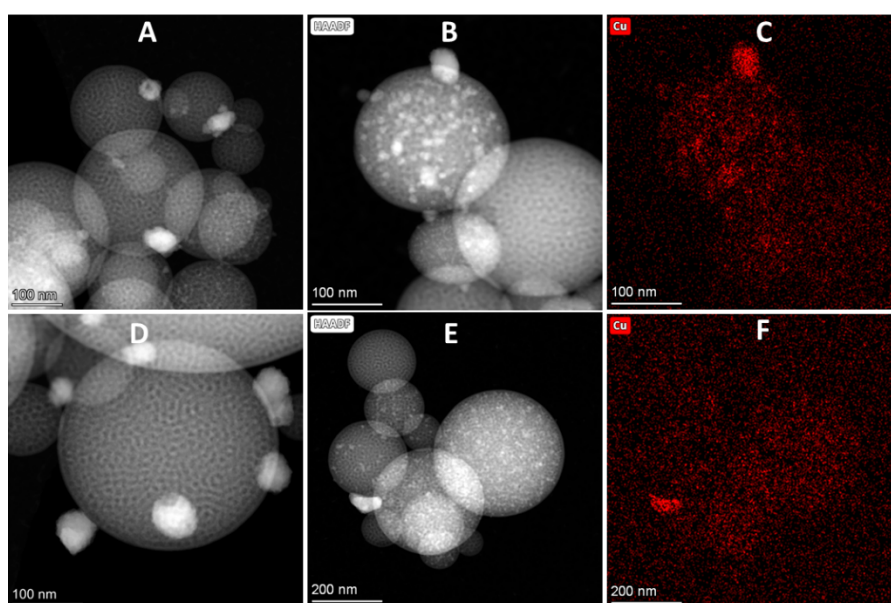


Figure S14: STEM comparison between 8h TOS (A, B, C) and 24h TOS (D, E; F) for 0.44O<sub>2</sub>. Panels A, B, D, E are acquired in dark field. Panels C, F are referred to the elemental mapping of Cu.

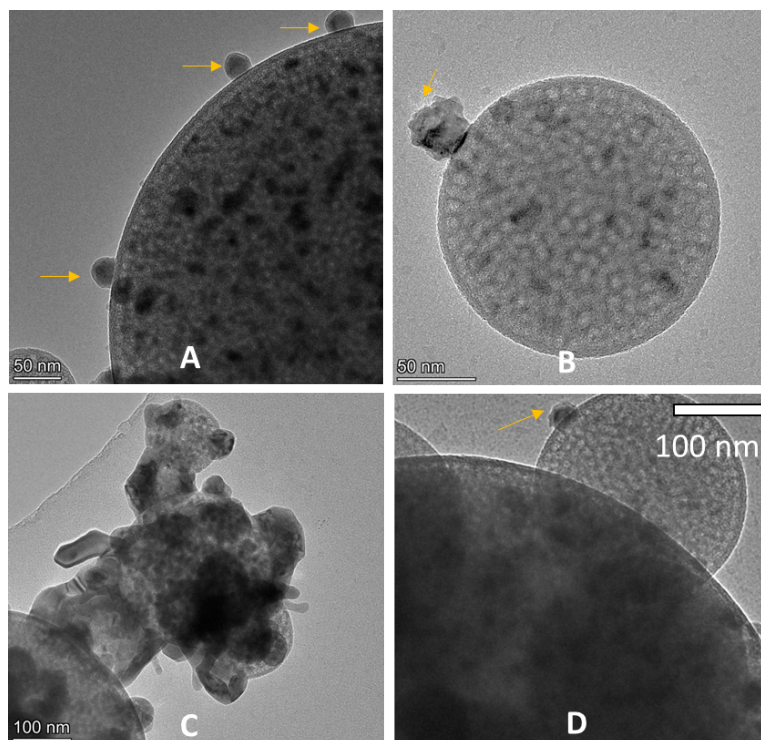


Figure S15: Carbonaceous deposit observed via TEM over different spent catalysts (TOS 24h). Panel A refers to NT, panel B refers to  $0.44\text{O}_2$ , panel C refers to  $1.77\text{O}_2$ , panel D refers to  $1.77\text{H}_2$ . TEM micrographs acquired in bright field.

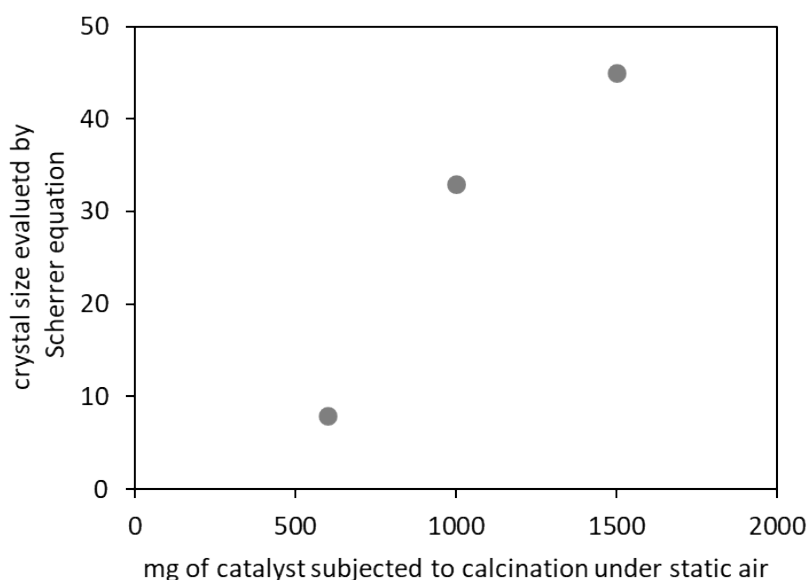


Fig. S16: relationship between the quantity of catalysts introduced in the crucible and subjected to calcination, and the corresponding crystal size evaluated by Scherrer equation after the calcination procedure. When introducing a lower amount of sample in the crucible, it is possible to avoid the formation of the largest CuO particles. This trend can be explained by changing the catalytic bed depth during calcination. According to Van Bekkum et al.

(zeolites, 7994, 14, 1994, R. A. Sheldon, H. Van Bekkum, Fine Chemicals through Heterogeneous Catalysis, 12, 2007, Wiley) water mobility is influenced by the depth of the

bed. The greater the depth, the more easily water vapor becomes trapped within the powders, accelerating metal diffusion related phenomena (and thus, sintering).

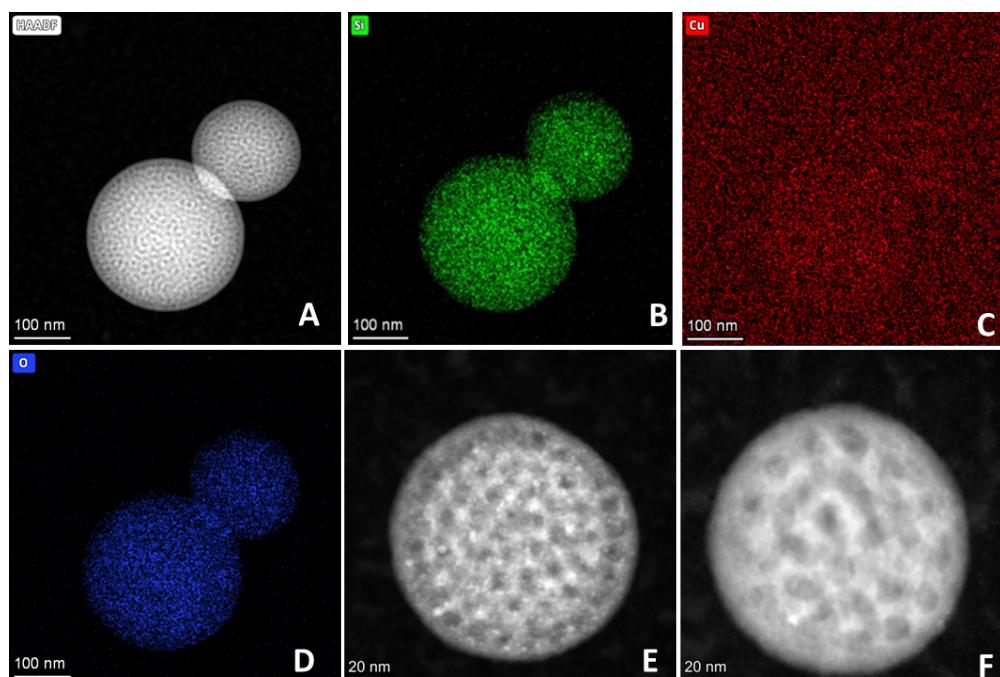


Figure S17: micrographs of Cu-SiO<sub>2</sub>-S: Panels A, E, F are acquired in dark field. Panels B, C, D refer to the elemental mapping of Si, Cu, O atoms.

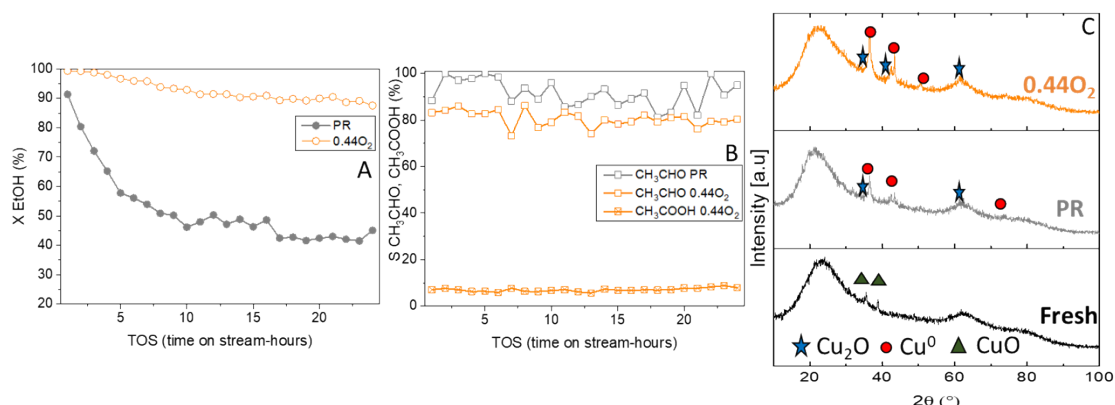


Figure S18: Ethanol conversion (A) and products selectivity (B) obtained over Cu-SiO<sub>2</sub>-S within 24 hours stability tests. 573 K, WHSV 4.02 h<sup>-1</sup>, constant ethanol feed, tot flow 120 mL/min. When oxygen is introduced in the feed, a correspondent reduction in the carbon balance has been observed: this can be due to concomitant formation of CO<sub>x</sub> (not quantified). Panel C refers to XRD patterns of fresh and spent catalysts.

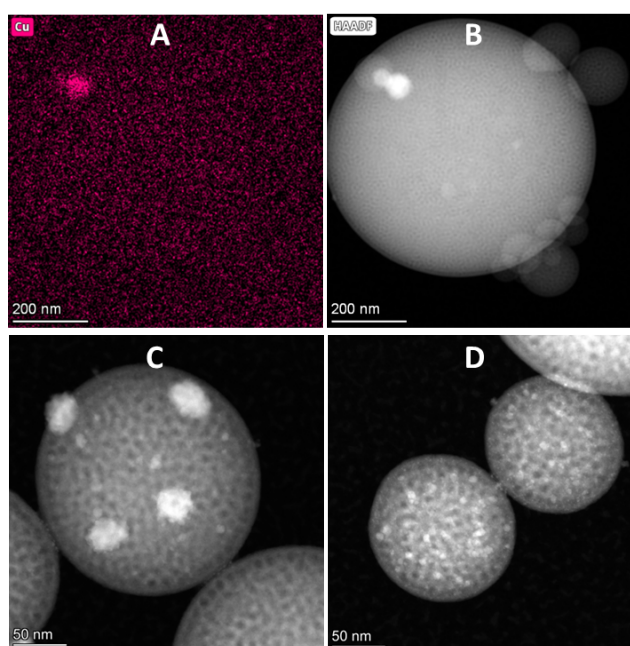


Figure S19: Panels A-D show spent  $0.44\text{O}_2$  (Cu-SiO<sub>2</sub>-S) after 24 hours TOS. Panel A is referred to STEM EDS elemental mapping of Cu atoms. Panels B, C, D refer to TEM micrographs acquired in dark field.